



1 **A Fast-response automated gas equilibrator (FaRAGE) for continuous *in situ***
2 **measurement of methane dissolved in water**

3 Shangbin Xiao¹, Liu Liu^{2*}, Wei Wang¹, Andreas Lorke^{1,3}, Jason Woodhouse² and Hans-Peter
4 Grossart^{2*}

5 ¹ College of Hydraulic & Environmental Engineering, China Three Gorges University, 443002 Yichang, China

6 ² Department of Experimental Limnology, Leibniz Institute of Freshwater Ecology and Inland Fisheries, 16775
7 Stechlin, Germany

8 ³ Institute for Environmental Sciences, University of Koblenz-Landau, 76829 Landau, Germany

9 *Corresponding authors

10 Emails: liu.liu@igb-berlin.de; grossart@igb-berlin.de

11 **Abstract**

12 Biogenic methane (CH₄) emissions from inland waters contribute substantially to
13 global warming. In aquatic systems, CH₄ dissolved in freshwater lakes and reservoirs is
14 highly heterogeneous both in space and time. To better understand the biological and physical
15 processes that affect sources and sinks of CH₄ in lakes and reservoirs, dissolved CH₄ needs to
16 be measured with a highest temporal resolution. To achieve this goal, we developed the **Fast-
17 Response Automated Gas Equilibrator (FaRAGE)** for real-time *in situ* measurement of
18 dissolved CH₄ concentration at the water surface and in the water column. FaRAGE can
19 achieve an exceptionally short response time (t_{95%} = 12 s when including the response time of
20 the gas analyzer) while retaining an equilibration ratio of 63% and a measurement accuracy of
21 0.5%. An equilibration ratio as high as 91.8% can be reached at the cost of a slightly
22 increased response time (16 s). The FaRAGE is capable of continuously measuring dissolved
23 CH₄ concentrations in the nM-to-mM (10⁻⁹ - 10⁻³ mol L⁻¹) range with a detection limit of sub-



24 nM (10^{-10} mol L⁻¹), when coupled with a cavity ring-down greenhouse gas analyzer (Picarro
25 GasScouter). It enables the possibility of mapping dissolved CH₄ concentration in a “quasi”
26 three-dimensional manner in lakes. The FaRAGE is simple to operate, inexpensive, and
27 suitable for continuous monitoring with a strong tolerance to suspended particles. The easy
28 adaptability to other gas analyzers such as Ultra-portable Los Gatos and stable isotopic gas
29 analyzer (Picarro G2132-i) also provides the potential for many further applications, e.g.
30 measuring dissolved ¹³C-CH₄ and CO₂.

31



32 **1 Introduction**

33 Despite the well-established perception of inland waters as a substantial source of
34 atmospheric methane (CH₄) (Bastviken et al., 2011; Cole et al., 2007; Tranvik et al., 2009),
35 large uncertainties remain owing to poorly constrained sources and sinks (Saunois et al.,
36 2019). Most freshwater lakes and reservoirs are often oversaturated with CH₄ (relative to
37 atmosphere) and its distribution is characterized by high spatio-temporal heterogeneities
38 (Hofmann, 2013). Point-based and short-term measurements can result in biases in estimating
39 diffusive CH₄ flux (Paranaíba et al., 2018). Thus, resolving the spatio-temporal dynamics of
40 dissolved CH₄ concentration in lake water is a prerequisite for better budgeting sources and
41 sinks in freshwater lakes.

42 Methane within lakes is often characterized by pronounced vertical and horizontal
43 concentration gradients, which can occur either below or above thermocline. In many deep
44 stratified lakes, a sharp vertical gradient below the thermocline can develop in the anoxic
45 hypolimnion (mM range) (Encinas Fernández et al., 2014; Liu et al., 1996). In contrast, in
46 some stratified lakes with a fully oxygenated hypolimnion CH₄ can accumulate above the
47 thermocline (~µM range) (Grossart et al., 2011; Donis et al., 2017; Günthel et al., 2019). The
48 concentration of dissolved CH₄ is also regulated by loss due to oxidation and emission to the
49 atmosphere (Bastviken et al., 2004; Juutinen et al., 2009). Both rates can be highly variable,
50 particularly for the flux term which is strongly affected by wind and convective mixing (Read
51 et al., 2012; Vachon and Prairie, 2013). In addition to the uneven vertical CH₄ distribution,
52 apparent horizontal gradients have been observed in lakes where littoral sediments are
53 identified as a CH₄ source (Murase et al., 2003). This horizontal CH₄ gradient can also
54 contribute to the epilimnetic CH₄ peak in pelagic waters via lateral transport (Hofmann et al.,
55 2010; Fernández et al., 2016; Murase et al., 2005; Peeters et al., 2019). Nevertheless,
56 dissolved CH₄ in lake water is not only featured with variable spatial patterns, it also changes



57 at different time scales as most processes that contribute to the spatial heterogeneity are not
58 always synchronized.

59 The rise and fall of lake CH₄ concentration often show strong seasonality that are
60 driven primarily by thermal stratification (Encinas Fernández et al., 2014) and phytoplankton
61 dynamics (Günthel et al., 2019). While the build-up of hypolimnetic CH₄ storage is a slow
62 process that is closely related to the development of lake hypoxia, the epilimnetic CH₄
63 maximum can be highly variable even at a daily basis as it is strongly affected by
64 phytoplankton dynamics (Günthel et al., 2019; Hartmann et al., 2020; Bižić et al., 2020). In
65 addition, storms can act as another driver for short-term CH₄ dynamics in the lake because it
66 often leads to higher evasion rates caused by strong vertical turbulent mixing (Zimmermann et
67 al., 2019) and enhanced horizontal transport (Fernández et al., 2016). While the seasonal
68 patterns of dissolved CH₄ concentration in lake water seem recurrent and can be simulated
69 (Bartosiewicz et al., 2019), the unpredictable effects of short-term phytoplankton dynamics
70 and storm events can present a challenge in modeling lake CH₄ dynamics.

71 While there is urgent need for resolving the spatio-temporal variabilities of CH₄ in
72 large water bodies (e.g. deep, stratified lakes), we recognize limitations in the available
73 methodology. Like most gases in dissolved phase, CH₄ cannot be measured directly in water.
74 Instead, a carrier gas (synthetic air or at air concentration) is added to achieve (full/partial)
75 gas-water equilibration. The headspace gas sample is then measured with a gas spectrometer
76 and the concentration of targeted gas can be calculated according to Henry's law (Magen et
77 al., 2014). To save sampling effort, continuous gas equilibration devices have been developed,
78 which generally can be classified to four categories: 1) Membrane type (Schlüter and Gentz,
79 2008; Boulart et al., 2010; Gonzalez-Valencia et al., 2014; Hartmann et al., 2018) - gases are
80 extracted from water by using a gas-permeable membrane; 2) Marble type (Frankignoulle et
81 al., 2001; Santos et al., 2012) - gas exchange is enhanced by pumping water through marbles



82 that increases the gas-water contact area; 3) Bubble type (Schneider et al., 1992; Körtzinger et
83 al., 1996; Gültow et al., 2011) - dissolved gases are stripped out by bubbling the water sample;
84 4) Showerhead type (Weiss-type) (Johnson, 1999; Rhee et al., 2009; Li et al., 2015) - water is
85 pumped from top and then mixed with a circulated headspace carrier gas. A full evaluation on
86 the performance of these devices was provided in a recent review (Webb et al., 2016), where,
87 the most important parameter, response time, was found to vary between 2-34 min for
88 dissolved CH₄. While it is already encouraging, improvements are expected to further shorten
89 the response time.

90 Driven by the need to resolve temporal and spatial variabilities of dissolved CH₄ in
91 lakes/reservoirs with sufficient precision, we developed a novel, low-cost equilibrator to
92 achieve fast gas-water equilibration. The **Fast-Response Automated Gas Equilibrator**
93 (**FaRAGE**) can be coupled with a portable gas analyzer, which makes it perfect for field use.
94 Here, the performance of the FaRAGE is evaluated by investigating its response time,
95 detection limit and equilibration ratio. Applications are provided exemplarily to demonstrate
96 the potential of the FaRAGE for improving our understanding on the spatial distribution and
97 temporal dynamics of dissolved CH₄ in inland waters.

98 **2 Materials and Methods**

99 **2.1 Device description**

100 The design of the FaRAGE is modified from two types of equilibrators: Bubble-type
101 (Schneider et al., 1992) and Weiss-type (Johnson, 1999). In contrast to the traditional bubble-
102 type and Weiss-type equilibrators that create a large-volume headspace and circulates air back
103 to the headspace, the FaRAGE is a flow-through system that adds gas flow into a constant
104 water flow to produce a minimal headspace for continuous concentration measurement of
105 CH₄ dissolved in water.

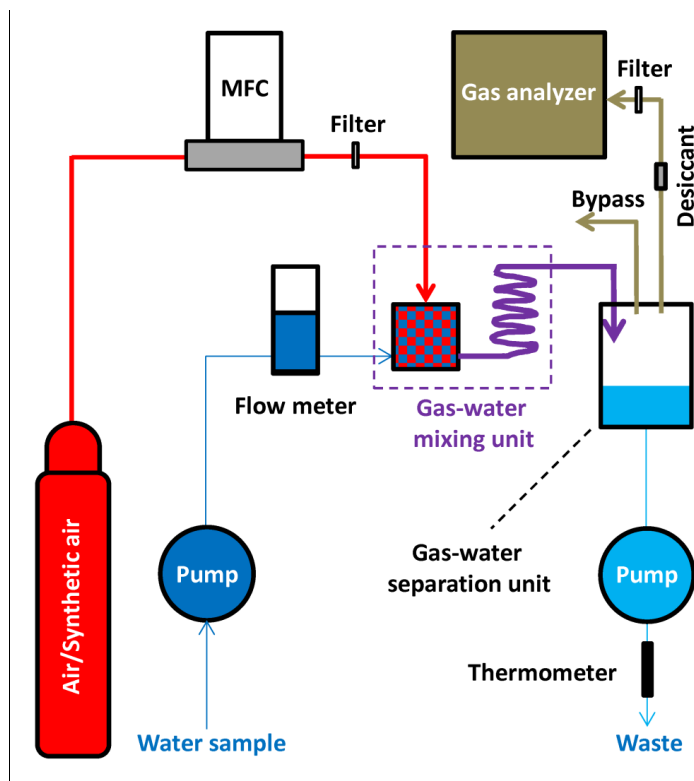


106 The operation principle of the FaRAGE is depicted in Fig. 1 and photos of the main
107 parts of the prototype are provided in Fig. S1. A list of information on suppliers and cost of
108 each part can be found in Table S1. A mass flow controller (SIERRA C50L, Netherlands) is
109 used to generate a constant carrier gas (normal air/synthetic air) flow (1 L min^{-1}) from a
110 compressed air tank coupled with a pressure regulator. Water samples are taken continuously
111 using a peristaltic pump (500 mL min^{-1}), and the flow is monitored using a flow meter
112 (Brooks Instrument, Germany). The two flows mix in a gas-water mixing unit that is
113 composed of a gas bubble generating unit and a coiled hose for further gas-water turbulent
114 mixing. In the bubble unit (modified from a 10 mL plastic syringe), a jet flow is created by
115 adapting narrowed tubing (2 mm inner diameter) to the water pumping hose (3.2 mm inner
116 diameter). Degassing occurs when the jet flow enters the chamber with a sudden enlarged
117 diameter (14 mm). Degassing is further enhanced by micro-bubbles that are generated by a
118 bubble diffuser attached to the carrier gas hose (inside the bubble unit). The gas-water
119 mixture flows through the 2-m long Tygon tube (3.2 mm inner diameter) where additional
120 equilibration occurs. The flow is finally introduced to a gas-water separation unit (a 30 mL
121 plastic syringe) where the headspace gas is separated from the water. In this chamber, water
122 falls down freely to the bottom while the headspace gas is taken directly to a greenhouse gas
123 analyzer (1 L min^{-1} gas pumping rate; GasScouter G4301, Picarro, USA). A 2-m long Tygon
124 tube (3.2 mm inner diameter) is attached to the top of the chamber for venting excess gas flow
125 while stabilizing gas pressure in the headspace. The bottom water is discharged back to the
126 lake using another peristaltic pump (500 mL min^{-1}). To protect the gas analyzer from
127 damaging high water vapor content, a Teflon membrane filter (pore size $0.2 \mu\text{m}$) is placed
128 before the gas intake (resulting in a $\sim 210 \text{ mL min}^{-1}$ reduction in flow rate of gas sample,
129 which is vented from the bypass at the top of the gas separation unit). A desiccant (a 20 mL
130 plastic syringe filled with dried silicone beads) is used to reduce moisture concentration to <
131 0.1% when attaching to a Picarro G2132-i isotope analyzer (Picarro, USA), in which < 1%



132 moisture level is required for ^{13}C - CH_4 measurement. The temperature of the water sample at
133 the point of equilibration with the headspace gas is monitored using a fast thermometer
134 (precision 0.001 °C, 1 Hz, TR-1050, RBR, Canada) attached to the end of water discharging
135 hose.

136 As concerns might arise from the availability of gas analyzer coupled to the FaRAGE,
137 in addition to Gas Scouter from Picarro, two additional widely used models of greenhouse gas
138 analyzers were tested. They are the Ultraportable Los Gatos (Los Gatos Research, USA) and
139 stable isotopic CH_4 analyzer (G2132-i, Picarro, USA). The main technical details of all three
140 tested gas analyzers are listed in Table S2.



141
142 **Fig. 1** Schematic design of the FaRAGE. The components include: Air tank containing
143 compressed carrier gas (air or synthetic air) with a pressure regulator, a mass flow controller



144 (MFC) for generating constant carrier gas flow, two peristaltic pumps for taking and
145 discharging water, respectively, a flow meter for monitoring water sample flow, a gas-water
146 mixing unit, a gas-water separation unit, a gas analyzer, and a thermometer for measuring
147 water temperature at phase equilibration. A Teflon membrane filter is placed after the MFC
148 and another is added before the gas analyzer to protect from being flooded. A desiccant is
149 used to dry the gas flow to the gas analyzer (if Picarro isotopic analyzer is used). The red
150 color marks the flow of carrier gas, dark blue line indicates the water sample, purple line
151 shows the flow of gas-water mixture, the light brown line shows the flow of gas sample (after
152 partial equilibration) and the light blue line depicts the water discharged back to lake. The
153 thickness of the lines scales with the gas/water flow rates. The arrows show the flow
154 directions.

155 **2.2 Lab validation**

156 The FaRAGE prototype was first tested intensively in the lab to determine both the
157 equilibration ratio and response time. The equilibration ratio is defined as the percentage of
158 the gaseous CH₄ concentrations at the outlet of the gas equilibrator in comparison to the
159 equilibrium concentration (full gas-water equilibration). The equilibration ratio was
160 established by measuring a range of CH₄ stock solutions (nano-to-micro molar dissolved gas
161 concentrations). These standard solutions were prepared by adding different amounts of CH₄
162 into a 200 mL headspace of a 2 L Schott bottle filled with Milli-Q water. The exact dissolved
163 CH₄ concentrations in these solutions were tested with the traditional manual headspace
164 method: a 400 mL headspace was created in a 500 mL plastic syringe with nitrogen gas. The
165 CH₄ concentration of the headspace gas was then measured using GasScouter G4301 (Picarro,
166 USA). At the same time, CH₄ concentrations of these standard solutions were measured with
167 the FaRAGE for at least 2 min and an average was calculated from more than 60 individual



168 data points. For simplicity, we directly compared dissolved CH₄ concentrations measured
169 using the two different methods, i.e., our equilibrator and manual headspace method.

170 The response time of the device was investigated by switching the water sample inlet
171 between two water samples with different CH₄ concentrations. Triplicated measurements
172 were performed. An exponential fit was applied to the concentration change curve and the
173 response time was determined as time needed to reach 95% of the final concentration.

174 The effect of water-to-gas mixing ratio on equilibration ratio and response time of the
175 device was investigated. By fixing the carrier gas flow rate to 1 L min⁻¹, the water-to-gas
176 mixing ratio was varied from 0.04, 0.08, 0.12, 0.15, 0.24, 0.29, 0.36, 0.43 and 0.5 by adjusting
177 the water sample flow rate. The effect of tube length on performance of the device was also
178 examined by adapting 1, 2, 4.4 and 8.4 m Tygon tube onto the gas-water mixing unit. For all
179 these tests, triplicated measurements of the equilibration ratio and response time were
180 performed corresponding to different mixing ratios and the mean values were used for
181 analysis.

182 Tests were performed to investigate the performance of the device when adapting to
183 two other types of gas analyzers. As the equilibration ratio is unaffected by the model of gas
184 analyzers, only response time was determined. This was done by fixing carrier gas and water
185 sample flow rates to 1 and 0.5 L min⁻¹, respectively. The surplus gas was vented to the air as
186 Ultraportable Los Gatos and Picarro G2132-i have a gas intake flow rate of only 500 and 25
187 mL min⁻¹, respectively. The effect of desiccant on response time of Picarro G2132-i was
188 checked by measuring gas samples with and without a desiccant installed.

189 **2.3 Field tests**

190 Two lakes in Germany were chosen for field test. Lake Stechlin is a deep meso-
191 oligotrophic lake with a maximum depth of 68 m and Lake Arend is a eutrophic lake with a



192 maximum depth of 48 m. Pronounced CH₄ peaks in the epilimnion of Lake Stechlin have
193 been previously reported that were measured with various methods (Grossart et al., 2011;
194 Hartmann et al., 2018; Tang et al., 2014). This makes it ideal for our testing purpose. While
195 CH₄ profiles at Lake Arend have never been reported, the metalimnetic oxygen minimum in
196 the lake observed during summer (Kreling et al., 2017) renders it interesting for CH₄ profiling
197 throughout the entire water column.

198 Due to the high potential of the FaRAGE for real-time *in situ* measurement of
199 dissolved CH₄ concentrations, we explored potential field applications. These field tests
200 included depth profiling of dissolved CH₄ concentrations in Lake Arend and Lake Stechlin
201 and investigations of the horizontal distribution of surface dissolved CH₄ concentration across
202 the entire Lake Stechlin. For the first application, a fast-response CTD (conductivity,
203 temperature and depth) profiler (XR-620 CTD+, RBR, Canada) was mounted onto a winch
204 with a 30 m long water hose (4 mm inner diameter) attached. The CTD profiler with hose was
205 lowered down continuously at a constant speed (1 m min⁻¹). The exact depth and temperature
206 of sampled water can be extracted from the CTD profiler by correcting for the travel time of
207 water sample flow in hose. For the spatial mapping, a GPS antenna (Taoglas, AA.162, USA)
208 was attached to the Picarro gas analyzer. The water intake was submerged 0.5 m below the
209 water surface together with the CTD profiler and fixed to one side of the boat. The boat was
210 driven at a constant speed of 5 km h⁻¹.

211 **2.4 Theoretical background and data processing**

212 The FaRAGE shares a similar working principle to the Weiss-type gas equilibrator
213 described by Johnson (1999). The theoretical background and equations are provided in S3.

214 A simplified calculation is described by referring to the manual headspace method. In
215 principle the gas-water mixture is analogous to the static headspace method with the final CH₄



216 concentration in the gas phase assumed to reach a full equilibrium with that dissolved in the
217 aqueous phase. Therefore, by specifying the mixing ratio of air and water, the total mass of
218 CH₄ can be calculated by summing up the CH₄ in the headspace with the dissolved CH₄ (at
219 equilibrium according to Henry's law, which is temperature and pressure dependent) in the
220 aqueous phase and subtracting the mass of background CH₄ (from carrying gas with known
221 concentration). The dissolved CH₄ concentration is then expressed as the volumetric
222 concentration of total net mass of CH₄ in the dissolved phase in the given sample volume. A
223 separated exemplary calculation sheet (excel file S5) is provided, which allows for correction
224 for temperature and pressure change.

225 As the equilibration is only partially reached (< 92%), a correction coefficient is
226 needed. This can be obtained by measuring the water samples with known concentrations
227 across a large gradient. By referring to the results measured with the manual headspace
228 method assuming full equilibration (Magen et al., 2014), an equation for precise correction of
229 the measured CH₄ concentrations can be obtained.

230 **3 Results and Discussion**

231 **3.1 Detection limit, equilibration ratio and response time**

232 The FaRAGE is capable of achieving a high gas equilibration ratio. We observed a
233 high correlation ($R^2 = 0.999$, $p < 0.01$) between the concentrations obtained using the
234 traditional headspace method and those measured using the FaRAGE (Fig. 2a) across a wide
235 range of dissolved CH₄ concentrations. The measurement accuracy is 0.5% (standard
236 deviation in relation to final concentration) once a stable plateau was reached (Fig. 2b). The
237 FaRAGE reaches a high equilibration ratio (63%) and ensures a rapid response. The
238 determined response time $t_{95\%}$ is only 12 s when switching from low-to-high (nano-to-micro
239 molar) dissolved CH₄ concentrations while the $t_{95\%}$ is a little longer (15 ± 2 s) when switching



240 from high-to-low concentration (Fig. 2b). For the current design specifications that allow for a
241 high equilibration ratio, the detection is theoretically limited by the sensitivity of the coupled
242 gas analyzer. In the lab tests, a clear response was observed at least for CH₄ concentration at
243 air saturation (16.9 nM inside the lab building). The measureable CH₄ concentrations should
244 be at least sub-nM (10⁻¹⁰ mol L⁻¹) given the high performance of cavity-ring-down gas
245 analyzers. This is more than sufficient for applications in inland waters where dissolved CH₄
246 concentrations are often above air saturation.

247 The response time for the FaRAGE results from two components: 1) the response of
248 the gas analyzer to changes in gas concentration and 2) the physical gas-water exchange
249 process. The response time for the gas analyzer is 5 s when the CH₄ concentration increases
250 (Fig. S2). The FaRAGE itself needs < 10 s to reach 95% of the final steady-state
251 concentration.

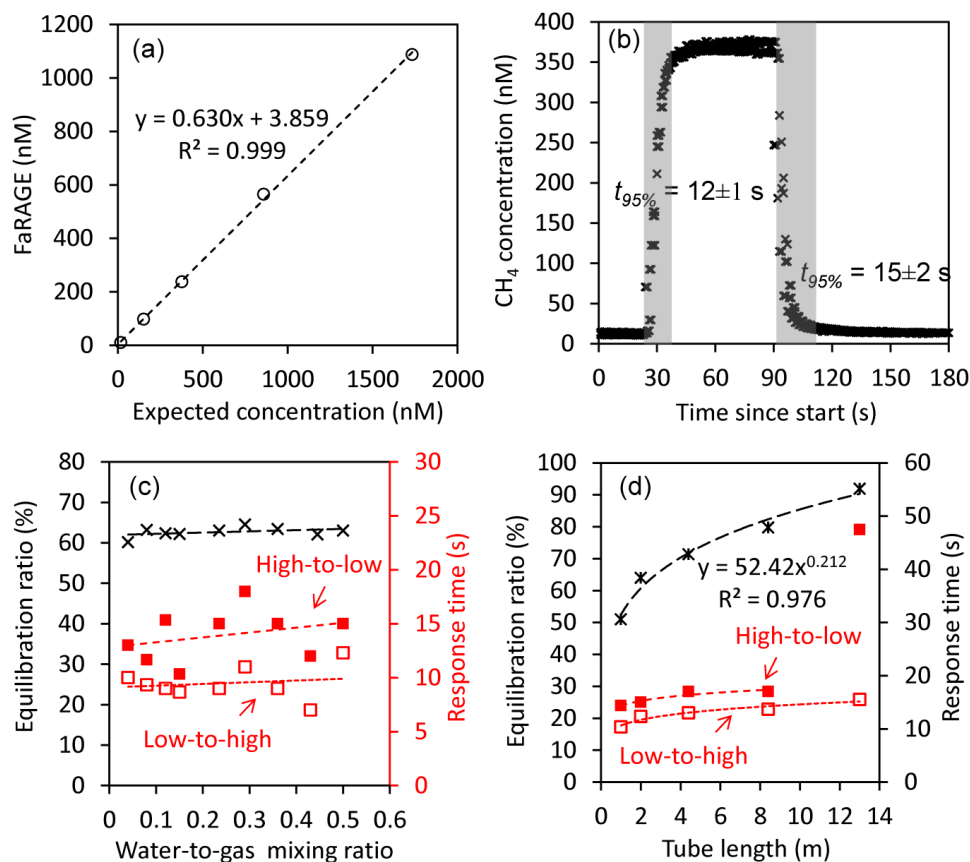
252 Equilibration ratio and response time of the FaRAGE is not sensitive to water-to-gas
253 mixing ratio (Fig. 2c) but rather to the length of the tube in the gas-water mixing unit (Fig. 2d).
254 Little effect was observed on the equilibration ratio in response to the increase of water-to-gas
255 mixing ratio. Also, the increase of water-to-gas mixing ratio did not significantly change the
256 response time of the device (on average 9 s for low-to-high and 13 s for high-to-low,
257 respectively). This is in contrast to other types of equilibrators in which an increase of water-
258 to-gas mixing ratio was found to result in a faster response (Webb et al., 2016). However, a
259 sharp enhancement of equilibration ratio was observed due to the extended length of the tube
260 for the gas-water mixing unit. A 91.8% equilibration ratio can be achieved by extending the
261 tube length to 13 m while extended response times (low-to-high 17 s and high-to-low 47.5 s,
262 respectively). Further enhancement of the equilibration ratio was not possible when a longer
263 tube (e.g. 18 m) was used. The gas flow rate cannot be stabilized at 1 L min⁻¹ due to the
264 increased resistance in response to the further extension of tube length.



265 As shown in Table S2 and Fig. S2, the fast response of the FaRAGE is partly due to
266 the extremely fast response of the Picarro Gas Scouter. This makes it unfair to compare with
267 other equilibrators in which different gas analyzers were used. Tests were performed by
268 adapting the FaRAGE to two other greenhouse gas analyzers (Ultraportable Los Gatos and
269 Picarro G2132-i) and the response times are listed in Table S3. Comparisons were made in
270 Webb et al. (2016) and Hartmann et al. (2018) where both CH₄ and ¹³C-CH₄ were measured
271 using a Picarro G2201-i (Picarro, USA). Here we used a similar Picarro stable isotopic gas
272 analyzer (Picarro G2132-i) and unified all previous reported response time τ to t_{95%} by
273 applying the equation t_{95%} = 3 τ . The comparison between up-to-date previous studies and this
274 study (Table S4) demonstrated the extraordinary fast response relative to all existing gas
275 equilibration devices. A 53 s response time was achieved when the FaRAGE was adapted to
276 the Picarro G2132-i, which is significantly faster than others (171-6744 s).



277



278

279 **Fig. 2** Performance of the Fast-Response Automated Gas Equilibrator (FaRAGE). (a)
280 Exemplary correlation between measurements with the FaRAGE (with a 2-m tube in the gas-
281 water mixing unit) and expected concentrations measured using the manual headspace method.
282 (b) Exemplary response time of FaRAGE for low-to-high and high-to-low concentration
283 changes (with a 2-m tube in the gas-water mixing unit; water-to-gas mixing ratio 0.5).
284 Triplicated tests were performed and averaged response time was taken at the time point when
285 95% of the final concentration was reached. (c) Equilibration ratio and response time in
286 response to changing water/gas mixing ratio (with a 2-m tube in the gas-water mixing unit).
287 Black cross symbols are equilibration ratios, and low-to-high and high-to-low response times
288 are represented by red open and solid squares, respectively. (d) Equilibration ratio and



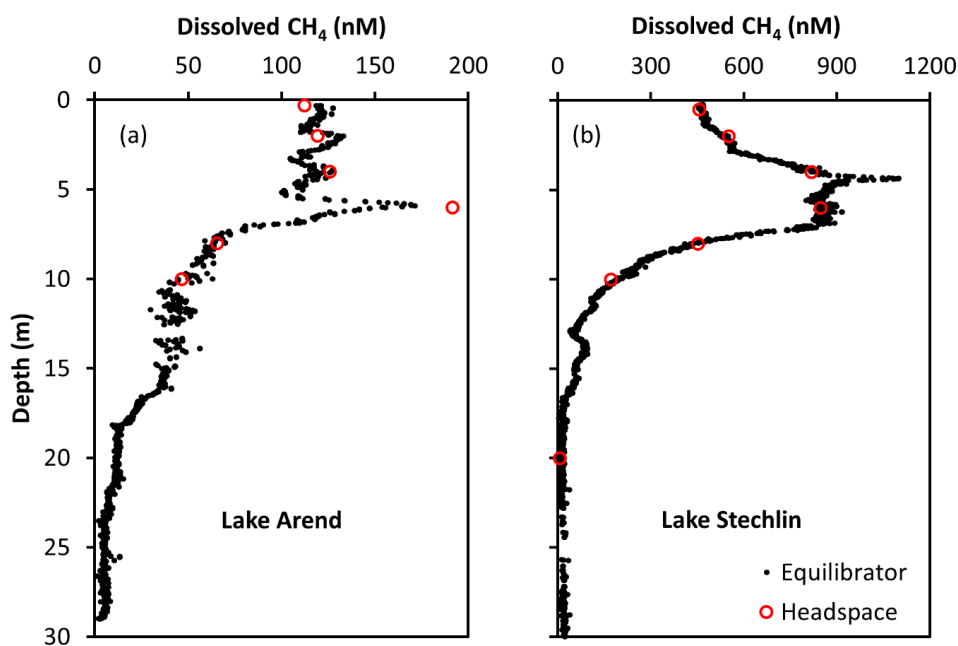
289 response time in response to changing tube length of gas-water mixing unit (with a fixed
290 water-to-gas mixing ratio of 0.5). Black cross symbols are equilibration ratios, and low-to-
291 high and high-to-low response times are represented by red open and solid squares,
292 respectively.

293 3.2 Depth profiles of dissolved CH₄ from multiple lakes

294 Good agreement was observed between depths profiles of dissolved CH₄ concentration
295 measured using two different methods (Fig. 3). The observed occurrence of a maximum in the
296 vertical profile of dissolved CH₄ concentration in the upper layer of Lake Stechlin (Fig. 3b) is
297 consistent with previous observations (Grossart et al., 2011; Tang et al., 2014; Hartmann et al.,
298 2018). In Lake Arend we also observed a CH₄ peak (Fig. 3a), although the overall
299 concentration was lower. In contrast, with the headspace method the FaRAGE allowed for the
300 localized CH₄ concentration maximum to be described at a high vertical resolution, similar to
301 that obtained with more sophisticated membrane filter equilibrators (Hartmann et al., 2018;
302 Gonzalez-Valencia et al., 2014). The FaRAGE was capable of resolving differences in
303 dissolved CH₄ concentration in lake water at decimeter scales with ease. Whilst care should
304 be taken to ensure the sampling hose moves smoothly and slowly through the water column,
305 continuous profiling of a 20 m deep lake can be completed in 30 min. This is a big advantage
306 since *in situ* CH₄ concentrations can vary at very short time scales (hours to days) subject to
307 internal production, oxidation, weather conditions and etc. (cf. Hartmann et al. (2020)).



308



309

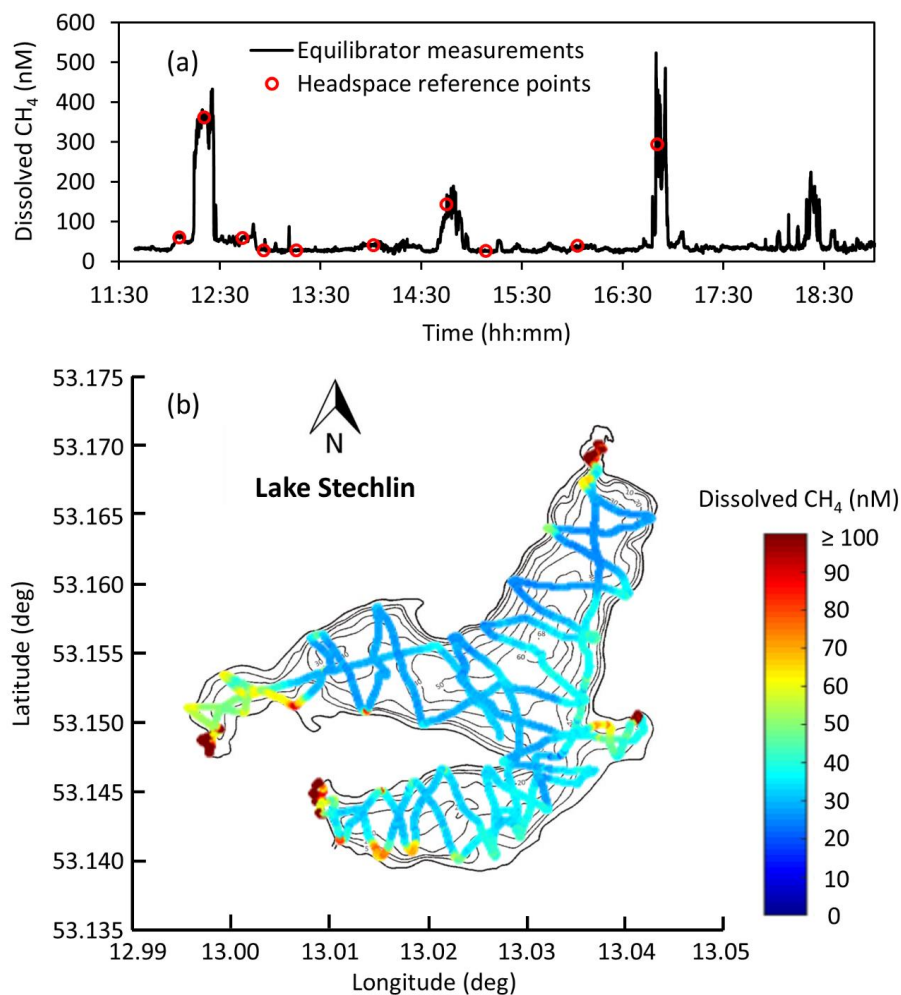
310 **Fig. 3** Depth profiles of dissolved CH₄ concentration from two lakes in Germany: (a)
311 eutrophic Lake Arend on June 17, 2019 and (b) meso-oligotrophic Lake Stechlin on July 23,
312 2019. Results from the headspace method are designated as red open circles and
313 measurements using the FaRAGE are shown as solid black dots.

314 3.3 Resolving spatial variabilities of dissolved CH₄ concentrations

315 We confirmed the capability of the FaRAGE to operate continuously over a 7-h period
316 without notable decreases in performance (Fig. 4a). Benefitting from its fast response rate,
317 surface water CH₄ concentrations across the 4.52 km² Lake Stechlin was mapped with great
318 detail within one day. During the cruise, 10 reference measurements were made at different
319 times, which were consistent with nonstop online *in situ* measurements. The cruising survey
320 demonstrated the capability of this device for resolving not just vertical dynamics of CH₄ in
321 lake water, but also the potential for studying horizontal distributions of CH₄ across large
322 distances, for instance large lakes and rivers. With a driving speed of 5 km h⁻¹ and a response



323 time of 12 s, a spatial resolution of 17 m can be achieved, which is sufficient for such a
324 medium-sized lake. The relative higher dissolved CH₄ concentrations in the shallow littoral
325 zone of Lake Stechlin (Fig. 4b) reflect higher CH₄ release from the local sediment.



326
327 **Fig. 4** Map of surface dissolved CH₄ concentration at Lake Stechlin. (a) Time series of 7-h
328 continuous surface water CH₄ measurement on March 28, 2019. The reference headspace
329 measurements are shown as red circles. (b) Spatial distribution of surface water CH₄
330 concentration is given on top of the lake's bathymetry. Colored symbols show CH₄



331 concentration according to the color bar. Black lines show the outline of the lake with depth
332 contours.

333 **4 Comments and Recommendations**

334 **4.1 Adaptability to different gas analyzers**

335 The reasons for the significantly shortened response time of the FaRAGE compared to
336 other types of gas equilibrators are two-fold. While the working principle of the FaRAGE is
337 based on the bubble-type (Schneider et al., 1992) and Weiss-type equilibrators (Johnson,
338 1999), a reduced headspace volume is adopted, which enhances the physical gas-water
339 exchange. Another reason is the use of extremely fast-response gas analyzer (Picarro Gas
340 Scouter 4301). It is a highly recommended combination for concentration measurement when
341 the best time-wise performance is preferred due to its great mobility (Table S2). However,
342 coupling to other Cavity-Ring-Down gas analyzers is also possible (Table S3). This feature
343 enables a possibility to investigate stable isotopic nature of dissolved CH₄, which is important
344 when sources of CH₄ need to be identified.

345 When a portable gas analyzer (Picarro Gas Scouter or Ultraportable Los Gatos) is used
346 for measuring CH₄ concentration only, the gas equilibrator can be optimized for different
347 application environments. The length of coiled tube for gas-water mixing can be adjusted to
348 change the response time (Fig. 2d). For smaller lakes a higher spatial resolution can be
349 obtained by shortening the equilibration tubing, which shortens the response time, and hence
350 increases the spatial resolution, whilst maintaining an acceptable equilibration ratio (51%
351 when tube length is 1 m). In environments with extremely low dissolved CH₄ concentrations,
352 e.g. ocean waters, a longer gas-water mixing tube should be used to ensure a high gas
353 equilibration ratio.



354 To measure stable isotopic CH₄ in water, the sensitivity of the FaRAGE can be
355 modified to better adapt to the choice of gas analyzer (e.g., when Picarro G2201-i or G2132-i
356 is used). For example, high dissolved CH₄ concentrations (e.g. μM-to-mM range) can be
357 measured with greater accuracy by increasing the flow rate of the carrier gas relative to the
358 sample water flow, therefore diluting the CH₄ concentrations to the range of the gas analyzer.
359 This can be particularly useful, for instance, when an instrument has an optimal precision at a
360 low concentration range (1.8-12 ppm for Picarro isotopic gas analyzer) for ¹³δC-CH₄
361 measurements. By using pure N₂ gas or carrier gases (e.g. Helium and Argon) and
362 corresponding gas analyzers, it would be possible to measure other dissolved gas
363 concentrations, e.g. CO₂ can be measured simultaneously (CO₂ was tested in this study, but
364 not shown for simplicity). In addition, benefited from the high equilibration ratio of this
365 device (max. 91.8%), it would be possible to measure dissolved CH₄ (and other gases) close
366 to equilibrium concentrations.

367 **4.2 Uncertainties due to suspended solids, temperature and pressure change**

368 The FaRAGE is proven to be resistant to suspended solids in freshwater lakes without
369 having to use additional accessories. As shown in Fig. S3, apparent phytoplankton blooms
370 were observed in the two studied lakes each with a high biomass (Chl-a > 30 μg L⁻¹) in the
371 epilimnetic water. The measurements were unaffected, without any interruptions during
372 measurements. As algal particles are a large component in freshwater systems, it is safe to
373 claim the resistance of this device to suspended solids in such a system. However, care must
374 be taken to avoid the water intake hose hitting the bottom sediment, which could cause
375 blockage of the water hose.

376 The temperature and hydrostatic pressure could both change when water is pumped
377 out through a water hose. To consider the temperature effect, a fast temperature logger is used



378 (Fig. 1) which allows for corrections in calculation. Instead of using *in situ* lake temperature,
379 the temperature measured at the gas equilibrator should be used where gas equilibration
380 occurs. Our measurements found a minor effect when measuring surface waters but an
381 apparent warming for hypolimnetic water in deep lakes. While a calibration can be done
382 directly by taking water samples from multiple depths of the lake (e.g., Fig. 3) to consider this
383 effect, one could make the calculation without taking many samples by applying temperature
384 correction.

385 The temperature correction can be made by referring to the manual headspace method.
386 The constant gas and water flow can be used as headspace and water volume, respectively. By
387 considering the temperature and pressure effects on gas solubility, the dissolved CH₄
388 concentrations can be calculated (an example calculation sheet is provided in Table S5). The
389 calibration curve can be established using the manual headspace measurements as standards.
390 The final concentrations can be corrected for partial equilibration by applying the equation
391 from the calibration curve (e.g., Fig. 2a). The response time should be deduced when
392 calculating CH₄ depth profiles and spatial distributions, in addition to the time lag caused by
393 pumping water samples by using an extended water hose.

394 **4.3 Calibration, maintenance and mobility**

395 The FaRAGE can be readily adopted for measuring other trace gases when coupled
396 with other portable gas analyzers. Due to differences in gas solubility (Duan and Sun, 2003;
397 Wiesenburg and Guinasso Jr, 1979), for each new gas, it would be necessary to establish the
398 relative equilibration efficiency and response time, following the approach we outlined here
399 for CH₄. Once set, a new calibration is only required when the tubing diameter or length is
400 changed (when the old one is filthy due to biofilm growth). This can be done by referring to a
401 number of known concentrations that covers a wide range (at least 5), e.g., taking water
402 samples from different water depth of the lake or a gradient from littoral to pelagic zones.



403 Once this full calibration is made, the calibration curve can be used for calculating the
404 subsequent measurements. A one-point reference measurement should be performed between
405 depth profiles or transects to check for apparent drifting. This can usually be done by taking
406 one surface water sample from a lake for manual headspace measurement. Care should be
407 taken when measuring in lakes with an anoxic hypolimnion where hydrogen sulfide is likely
408 to accumulate. The performance of Cavity-Ring-Down gas analyzers can be potential affected
409 by organics, ammonia, ethane, ethylene, or sulfur containing compounds (Kohl et al., 2019).
410 At these sites, it is always recommended to take additional samples and measure them with
411 traditional methods (e.g., with a Gas Chromatograph Analyzer).

412 The gas equilibrator should be carefully maintained. Replacement of parts is
413 recommended at a monthly basis provided the device is heavily in use. They include bubble
414 diffusor and the coiled gas-water mixing tube. In addition, to ensure the performance and
415 prevent biofilm formation the gas-water mixing and separation units should be cleaned after
416 use. Running with distilled or Milli-Q water would help to rinse the device and reduce the risk
417 of biofilm development in the inner tubes. The performance of peristaltic pumps should be
418 also regularly checked and the inner pump tubes need to be replaced to ensure a constant
419 water flow.

420 The combination of FaRAGE with the Picarro Gas Scouter provides the most mobility.
421 The system can be easily carried by one person and work in a small aluminum or inflatable
422 boat with a maximum capacity of three people is possible. The device can also work in bad
423 weather with additional measures based on protecting the gas analyzer from water damage by
424 rain or flooding.

425 **Code availability**

426 Not applicable.



427 **Data Availability**

428 An example calculation sheet (raw data of Fig. 2a) is provided as part of supporting
429 information for device calibration and for temperature and pressure correction when
430 calculating dissolved methane concentration. The full data sets associated with lab and field
431 tests are available upon request.

432 **Supplement link**

433 From Copernicus.

434 **Author contributions**

435 SBX and WW proposed the idea and built the first prototype. LL improved the
436 prototype and conducted lab and field tests. JW contributed to the field tests. AL contributed
437 to the derivation of equations; HPG advised the development of the modified prototype. LL
438 drafted the initial manuscript. All authors discussed the results and commented on the
439 manuscript.

440 **Competing interests**

441 The authors declare that they have no conflict of interest.

442 **Acknowledgements**

443 This work was financially supported by the National Natural Science Foundation of
444 China (grant No. 51979148) and Natural Science Foundation of Hubei Province, China
445 (2014CFB672). L.L., J.W. and H.P.G. were financially supported by the German Research
446 Foundation (DFG GR1540/21-1+2). The authors would like to thank Hannah Geisinger and
447 Truls Hveem Hansson for helping collecting field data.

448 **References**



- 449 Bartosiewicz, M., Przytulska, A., Lapierre, J. F., Laurion, I., Lehmann, M. F., and Maranger,
450 R.: Hot tops, cold bottoms: Synergistic climate warming and shielding effects increase carbon
451 burial in lakes, *Limnol. Oceanogr. Lett.*, 4, 132-144, <https://doi.org/10.1002/lol2.10117>, 2019.
- 452 Bastviken, D., Cole, J., Pace, M., and Tranvik, L.: Methane emissions from lakes:
453 Dependence of lake characteristics, two regional assessments, and a global estimate, *Global*
454 *Biogeochem. Cy.*, 18, <https://doi.org/10.1029/2004GB002238>, 2004.
- 455 Bastviken, D., Tranvik, L. J., Downing, J. A., Crill, P. M., and Enrich-Prast, A.: Freshwater
456 methane emissions offset the continental carbon sink, *Science*, 331, 50-50,
457 <https://doi.org/10.1126/science.1196808>, 2011.
- 458 Bižić, M., Klintzsch, T., Ionescu, D., Hindiyeh, M. Y., Günthel, M., Muro-Pastor, A. M.,
459 Eckert, W., Urich, T., Keppler, F., and Grossart, H.-P.: Aquatic and terrestrial cyanobacteria
460 produce methane, *Sci. Adv.*, 6, eaax5343, <https://doi.org/10.1126/sciadv.aax5343>, 2020.
- 461 Boulart, C., Connelly, D., and Mowlem, M.: Sensors and technologies for in situ dissolved
462 methane measurements and their evaluation using Technology Readiness Levels, *Trends Anal.*
463 *Chem.*, 29, 186-195, <https://doi.org/10.1016/j.trac.2009.12.001>, 2010.
- 464 Cole, J. J., Prairie, Y. T., Caraco, N. F., McDowell, W. H., Tranvik, L. J., Striegl, R. G.,
465 Duarte, C. M., Kortelainen, P., Downing, J. A., and Middelburg, J. J.: Plumbing the global
466 carbon cycle: integrating inland waters into the terrestrial carbon budget, *Ecosystems*, 10,
467 172-185, <https://doi.org/10.1007/s10021-006-9013-8>, 2007.
- 468 Donis, D., Flury, S., Stöckli, A., Spangenberg, J. E., Vachon, D., and McGinnis, D. F.: Full-
469 scale evaluation of methane production under oxic conditions in a mesotrophic lake, *Nat.*
470 *Commun.*, 8, 1661, <https://doi.org/10.1038/s41467-017-01648-4>, 2017.
- 471 Duan, Z., and Sun, R.: An improved model calculating CO₂ solubility in pure water and
472 aqueous NaCl solutions from 273 to 533 K and from 0 to 2000 bar, *Chem. Geol.*, 193, 257-
473 271, [https://doi.org/10.1016/S0009-2541\(02\)00263-2](https://doi.org/10.1016/S0009-2541(02)00263-2), 2003.



474 Encinas Fernández, J., Peeters, F., and Hofmann, H.: Importance of the autumn overturn and
475 anoxic conditions in the hypolimnion for the annual methane emissions from a temperate lake,
476 *Environ. Sci. Technol.*, 48, 7297-7304, <https://doi.org/10.1021/es4056164>, 2014.

477 Fernández, J. E., Peeters, F., and Hofmann, H.: On the methane paradox: Transport from
478 shallow water zones rather than in situ methanogenesis is the major source of CH₄ in the open
479 surface water of lakes, *J. Geophys. Res.: Biogeosciences*, 121, 2717-2726,
480 <https://doi.org/10.1002/2016JG003586>, 2016.

481 Frankignoulle, M., Borges, A., and Biondo, R.: A new design of equilibrator to monitor
482 carbon dioxide in highly dynamic and turbid environments, *Water Res.*, 35, 1344-1347,
483 [https://doi.org/10.1016/S0043-1354\(00\)00369-9](https://doi.org/10.1016/S0043-1354(00)00369-9), 2001.

484 Gonzalez-Valencia, R., Magana-Rodriguez, F., Gerardo-Nieto, O., Sepulveda-Jauregui, A.,
485 Martinez-Cruz, K., Walter Anthony, K., Baer, D., and Thalasso, F.: In situ measurement of
486 dissolved methane and carbon dioxide in freshwater ecosystems by off-axis integrated cavity
487 output spectroscopy, *Environ. Sci. Technol.*, 48, 11421-11428,
488 <https://doi.org/10.1021/es500987j>, 2014.

489 Grossart, H.-P., Frindte, K., Dziallas, C., Eckert, W., and Tang, K. W.: Microbial methane
490 production in oxygenated water column of an oligotrophic lake, *Proc. Natl. Acad. Sci.*, 108,
491 19657-19661, <https://doi.org/10.1073/pnas.1110716108>, 2011.

492 Gülzow, W., Rehder, G., Schneider, B., Deimling, J. S. v., and Sadkowiak, B.: A new method
493 for continuous measurement of methane and carbon dioxide in surface waters using off-axis
494 integrated cavity output spectroscopy (ICOS): An example from the Baltic Sea, *Limnol.*
495 *Oceanogr.: Methods*, 9, 176-184, <https://doi.org/10.4319/lom.2011.9.176>, 2011.

496 Günthel, M., Donis, D., Kirillin, G., Ionescu, D., Bizic, M., McGinnis, D. F., Grossart, H.-P.,
497 and Tang, K. W.: Contribution of oxic methane production to surface methane emission in
498 lakes and its global importance, *Nat. Commun.*, 10, 1-10, [https://doi.org/10.1038/s41467-019-](https://doi.org/10.1038/s41467-019-13320-0)
499 13320-0, 2019.



500 Hartmann, J. F., Gentz, T., Schiller, A., Greule, M., Grossart, H. P., Ionescu, D., Keppler, F.,
501 Martinez-Cruz, K., Sepulveda-Jauregui, A., and Isenbeck-Schröter, M.: A fast and sensitive
502 method for the continuous in situ determination of dissolved methane and its $\delta^{13}\text{C}$ -isotope
503 ratio in surface waters, *Limnol. Oceanogr.: Methods*, 16, 273-285,
504 <https://doi.org/10.1002/lom3.10244>, 2018.

505 Hartmann, J. F., Gunthel, M., Klintzsch, T., Kirillin, G., Grossart, H.-P., Keppler, F., and
506 Isenbeck-Schröter, M.: High Spatio-Temporal Dynamics of Methane Production and
507 Emission in Oxidic Surface Water, *Environ. Sci. Technol.*, 54, 1451-1463,
508 <https://doi.org/10.1021/acs.est.9b03182>, 2020.

509 Hofmann, H., Federwisch, L., and Peeters, F.: Wave-induced release of methane: Littoral
510 zones as source of methane in lakes, *Limnol. Oceanogr.*, 55, 1990-2000,
511 <https://doi.org/10.4319/lo.2010.55.5.1990>, 2010.

512 Hofmann, H.: Spatiotemporal distribution patterns of dissolved methane in lakes: How
513 accurate are the current estimations of the diffusive flux path?, *Geophys. Res. Lett.*, 40, 2779-
514 2784, <https://doi.org/10.1002/grl.50453>, 2013.

515 Johnson, J. E.: Evaluation of a seawater equilibrators for shipboard analysis of dissolved
516 oceanic trace gases, *Anal. Chim. Acta*, 395, 119-132, [https://doi.org/10.1016/S0003-](https://doi.org/10.1016/S0003-2670(99)00361-X)
517 2670(99)00361-X, 1999.

518 Juutinen, S., Rantakari, M., Kortelainen, P., Huttunen, J. T., Larmola, T., Alm, J., Silvola, J.,
519 and Martikainen, P. J.: Methane dynamics in different boreal lake types, *Biogeosciences*, 6,
520 209–223, <https://doi.org/10.5194/bg-6-209-2009>, 2009.

521 Kohl, L., Koskinen, M., Rissanen, K., Haikarainen, I., Polvinen, T., Hellén, H., and Pihlatie,
522 M.: Interferences of volatile organic compounds (VOCs) on methane concentration
523 measurements, *Biogeosciences*, 16, 3319-3332, <https://doi.org/10.5194/bg-16-3319-2019>,
524 2019.



- 525 Körtzinger, A., Thomas, H., Schneider, B., Gronau, N., Mintrop, L., and Duinker, J. C.: At-
526 sea intercomparison of two newly designed underway pCO₂ systems - encouraging results,
527 *Mar. Chem.*, 52, 133-145, [https://doi.org/10.1016/0304-4203\(95\)00083-6](https://doi.org/10.1016/0304-4203(95)00083-6), 1996.
- 528 Kreling, J., Bravidor, J., Engelhardt, C., Hupfer, M., Koschorreck, M., and Lorke, A.: The
529 importance of physical transport and oxygen consumption for the development of a
530 metalimnetic oxygen minimum in a lake, *Limnol. Oceanogr.*, 62, 348-363,
531 <https://doi.org/10.1002/lno.10430>, 2017.
- 532 Li, Y., Zhan, L., Zhang, J., and Chen, L.: Equilibrator-based measurements of dissolved
533 methane in the surface ocean using an integrated cavity output laser absorption spectrometer,
534 *Acta Oceanol. Sin.*, 34, 34-41, <https://doi.org/10.1007/s13131-015-0685-9>, 2015.
- 535 Liu, R., Hofmann, A., Gülaçar, F. O., Favarger, P.-Y., and Dominik, J.: Methane
536 concentration profiles in a lake with a permanently anoxic hypolimnion (Lake Lugano,
537 Switzerland-Italy), *Chem. Geol.*, 133, 201-209, [https://doi.org/10.1016/S0009-2541\(96\)00090-3](https://doi.org/10.1016/S0009-2541(96)00090-3), 1996.
- 538
- 539 Magen, C., Lapham, L. L., Pohlman, J. W., Marshall, K., Bosman, S., Casso, M., and
540 Chanton, J. P.: A simple headspace equilibration method for measuring dissolved methane,
541 *Limnol. Oceanogr.: Methods*, 12, 637-650, <https://doi.org/10.4319/lom.2014.12.637>, 2014.
- 542 Murase, J., Sakai, Y., Sugimoto, A., Okubo, K., and Sakamoto, M.: Sources of dissolved
543 methane in Lake Biwa, *Limnology*, 4, 91-99, <https://doi.org/10.1007/s10201-003-0095-0>,
544 2003.
- 545 Murase, J., Sakai, Y., Kametani, A., and Sugimoto, A.: Dynamics of methane in mesotrophic
546 Lake Biwa, Japan, *Ecol. Res.* 20, 377-385, <https://doi.org/10.1007/s11284-005-0053-x>, 2005.
- 547 Paranaíba, J. R., Barros, N., Mendonça, R., Linkhorst, A., Isidorova, A., Roland, F. b.,
548 Almeida, R. M., and Sobek, S.: Spatially resolved measurements of CO₂ and CH₄
549 concentration and gas-exchange velocity highly influence carbon-emission estimates of
550 reservoirs, *Environ. Sci. Technol.*, 52, 607-615, <https://doi.org/10.1021/acs.est.7b05138>, 2018.



- 551 Peeters, F., Fernandez, J. E., and Hofmann, H.: Sediment fluxes rather than oxic
552 methanogenesis explain diffusive CH₄ emissions from lakes and reservoirs, *Sci. Rep.*, 9,
553 <https://doi.org/10.1038/s41598-018-36530-w>, 2019.
- 554 Read, J. S., Hamilton, D. P., Desai, A. R., Rose, K. C., MacIntyre, S., Lenters, J. D., Smyth, R.
555 L., Hanson, P. C., Cole, J. J., and Staehr, P. A.: Lake-size dependency of wind shear and
556 convection as controls on gas exchange, *Geophys. Res. Lett.*, 39,
557 <https://doi.org/10.1029/2012GL051886>, 2012.
- 558 Rhee, T., Kettle, A., and Andreae, M.: Methane and nitrous oxide emissions from the ocean:
559 A reassessment using basin-wide observations in the Atlantic, *J. Geophys. Res.: Atmospheres*,
560 114, <https://doi.org/10.1029/2008JD011662>, 2009.
- 561 Santos, I. R., Maher, D. T., and Eyre, B. D.: Coupling automated radon and carbon dioxide
562 measurements in coastal waters, *Environ. Sci. Technol.*, 46, 7685-7691,
563 <https://doi.org/10.1021/es301961b>, 2012.
- 564 Saunio, M., Stavert, A. R., Poulter, B., et al.: The Global Methane Budget 2000–2017, *Earth*
565 *Syst. Sci. Data Discuss.*, <https://doi.org/10.5194/essd-2019-128>, in review, 2019.
- 566 Schlüter, M., and Gentz, T.: Application of membrane inlet mass spectrometry for online and
567 in situ analysis of methane in aquatic environments, *J. Am. Soc. Mass Spectrom.*, 19, 1395-
568 1402, <https://doi.org/10.1016/j.jasms.2008.07.021>, 2008.
- 569 Schneider, B., Kremling, K., and Duinker, J. C.: CO₂ partial pressure in Northeast Atlantic
570 and adjacent shelf waters: Processes and seasonal variability, *J. Marine Syst.*, 3, 453-463,
571 [https://doi.org/10.1016/0924-7963\(92\)90016-2](https://doi.org/10.1016/0924-7963(92)90016-2), 1992.
- 572 Tang, K. W., McGinnis, D. F., Frindte, K., Brüchert, V., and Grossart, H.-P.: Paradox
573 reconsidered: Methane oversaturation in well-oxygenated lake waters, *Limnol. Oceanogr.*, 59,
574 275-284, <https://doi.org/10.4319/lo.2014.59.1.0275>, 2014.
- 575 Tranvik, L. J., Downing, J. A., Cotner, J. B., Loiselle, S. A., Striegl, R. G., Ballatore, T. J.,
576 Dillon, P., Finlay, K., Fortino, K., and Knoll, L. B.: Lakes and reservoirs as regulators of



- 577 carbon cycling and climate, *Limnol. Oceanogr.*, 54, 2298-2314,
578 https://doi.org/10.4319/lo.2009.54.6_part_2.2298, 2009.
- 579 Vachon, D., and Prairie, Y. T.: The ecosystem size and shape dependence of gas transfer
580 velocity versus wind speed relationships in lakes, *Can. J. Fish. Aquat. Sci.*, 70, 1757-1764,
581 <https://doi.org/10.1139/cjfas-2013-0241>, 2013.
- 582 Webb, J. R., Maher, D. T., and Santos, I. R.: Automated, in situ measurements of dissolved
583 CO₂, CH₄, and $\delta^{13}\text{C}$ values using cavity enhanced laser absorption spectrometry: Comparing
584 response times of air-water equilibrators, *Limnol. Oceanogr.: Methods*, 14, 323-337,
585 <https://doi.org/10.1002/lom3.10092>, 2016.
- 586 Wiesenburg, D. A., and Guinasso Jr, N. L.: Equilibrium solubilities of methane, carbon
587 monoxide, and hydrogen in water and sea water, *J. Chem. Eng. Data*, 24, 356-360,
588 <https://doi.org/10.1021/je60083a006>, 1979.
- 589 M. Zimmermann, M. J. Mayr, D. Bouffard, W. Eugster, T. Steinsberger, B. Wehrli, A. Brand,
590 and Bürgmann H.: Lake overturn as a key driver for methane oxidation, *bioRxiv*,
591 <https://doi.org/10.1101/689182>, 2019.